Research Article

Synthesis and Characterization of One-Dimensional Porous (Zn,Cd)S/SiO$_2$ Composite Nanostructural Materials

Xiuli Fu,[1] Guijun Ban,[1] Dan Li,[1,2] Hanyuan Chen,[2] and Zhijian Peng[2]

[1] *School of Science, Beijing University of Posts and Telecommunications, Beijing 100876, China*
[2] *School of Engineering and Technology, China University of Geosciences, Beijing 100083, China*

Correspondence should be addressed to Xiuli Fu; xiulifu@bupt.edu.cn and Zhijian Peng; pengzhijian@cugb.edu.cn

One-dimensional (1D) porous (Zn,Cd)S/SiO$_2$ composite nanostructural materials were synthesized by thermal evaporation of ZnS and CdS mixture powder at 950°C. The nanomaterials were collected from silicon wafers which were coated with 10 nm thick gold and were set apart from the source about 10 cm away. The diameter of the as-prepared 1D porous composite nanostructures is in the range of 1–1.5 μm and their lengths are up to tens to hundreds of micrometers. The photoluminescence spectra measured at different temperatures of the prepared nanostructures display a similar broadband signature, which can be fitted by Gaussian function into three emission peaks centered at 477, 536, and 588 nm and attributed to band edge emission, neutral oxygen vacancies, and antisymmetric stretching of Si–O–Si and nonstoichiometric SiO$_x$ ($1 < x < 2$), respectively.

1. Introduction

Recently, one-dimensional (1D) nanostructural materials, such as nanotubes, nanowires, and nanobelts, have attracted much attention due to their intriguing properties. II–VI semiconductors with energy gaps covering the visible spectral range are excellent candidates for optoelectronic devices. In the past decade, considerable effort has been put into the synthesis of 1D II–VI semiconductor nanostructures using metal-organic chemical vapor deposition [1], vapor transport method [2–4], solution [5], solvothermal method, [6] and others [7, 8], because of their wide applications in optoelectronic [9], electronics [1], sensory nanotechnology [10, 11], and so on. In particular, ternary chalcogenide semiconductors, such as Zn-Cd-E (E = S, Se), are of special interest due to their possibility of fine tuning of electronic properties through changing the atomic ratio of Cd to Zn. For example, (Zn,Cd)S, a ternary chalcogenide semiconductor, has a variable band-gap energy from 2.4 to 3.7 eV, primarily dependent on the relative atomic ratio of Cd to Zn. So, ternary chalcogenide materials have attracted renewed interest for applications in nanoelectronics and photonics [9], photovoltaic and chemical sensing devices [11], laser [12], and

UV-A sensor [13]. In this paper, we report a simple and cost-effective way to fabricate 1D porous tube-like (Zn,Cd)S/SiO$_2$ composite nanostructural materials by thermal evaporation.

2. Experimental

A home-designed rapid heating tube furnace was used for the synthesis of materials. A quartz tube with an outer diameter of 40 mm, inner diameter of 36 mm, and length of 1400 mm was installed in the furnace, and another quartz tube with an outer diameter of 34 mm, inner diameter of 32 mm, and length of 1000 mm was installed in the larger quartz tube, in order to protect the larger quartz tube from pollution damage during experiments.

One gram ZnS and CdS powders (ZnS : CdS = 1 : 10 in mass) were fully mixed and loaded into a ceramic boat, and then the boat was transported into the smaller quartz tube and set in the center of the constant high-temperature zone of the furnace. The substrate, which was silicon wafers deposited with a thin film of gold (~10 nm) by magnetron sputtering in advance, was set in the quartz tube with a distance of 10 cm away from the source on the downstream
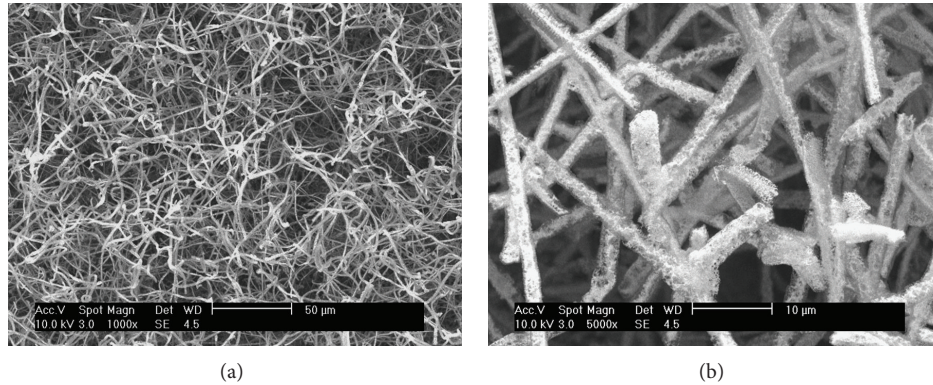
(a)

(b)

Figure 1: Low-magnification (a) and high-magnification (b) SEM images of the as-synthesized products.

of the system. The system was then pumped out up to about 200 Pa by a mechanical rotary pump. After evacuating the residual air and venting with high-purity N_2 (99.99%) into the tube for several times, trying to eliminate most of the oxygen in the tube, the furnace was heated up to 950°C in 1 h and held for 10 min before it was cooled down to room temperature naturally. During the whole synthesis process of nanomaterials, high-purity N_2 was introduced into the tube at a constant flow rate of 30 sccm (standard cubic centimeters per minute), and the mechanical rotary pump keeps running to maintain the system pressure at about 200 Pa. Finally, a white wool-like product was obtained.

The general morphology of the products was examined by scanning electron microscope (SEM, Hitachi X650). Detailed microstructure analysis was carried out using transmission electron microscopy (TEM, FEI Tecnai G2 F20 U-TWIN) with a GIF Tridiem CCD camera operating at 200 KV. The chemical composition was identified by an energy dispersive X-ray (EDX) spectrometer attached to the TEM microscope. The photoluminescence (PL) spectrum was recorded using a He-Cd laser (442 nm) as excitation source.

3. Results and Discussion

3.1. Morphology, Composition, and Structure. Figure 1 shows the SEM images of the white wool-like products deposited onto a Si wafer which was placed from the source about 10 cm away with corresponding temperature of 820–790°C. From Figure 1(a), one can easily find that the materials can be synthesized in mass production and have a wire-like feature. On checking tens of nanostructures, the diameter of the wires was in the range of 1–1.5 μm, and the lengths of the products were up to tens to hundreds of micrometers.

From the high-magnification SEM image shown in Figure 1(b), it could be clearly observed that each single nanostructure has a uniform diameter along its length, and it is porous. Also we can observe that there is a great contrast in the single porous wire-like structure which might be attributed to the composition difference and will be further presented in the following.

Figure 2 illustrates the TEM results of the as-synthesized 1D porous wire-like nanostructure. Figure 2(a) is a typical TEM image of a single 1D porous wire-like nanostructure. The great contrast in the radial direction of the nanostructure seems to indicate that the nanostructures are of cable-like or tube-like structure. It was measured from TEM images that this nanostructure has a diameter of about 1 micrometer with a shell of approximately 200 nanometers in thickness. This image also confirms the porosity of the nanostructures which was observed in SEM examination as shown in Figure 1.

The composition and structure of different areas of distinct contrast were characterized by EDS and high-resolution TEM (HRTEM). The EDS spectra taken from the areas as indicated in squares I and II in Figure 2(a) are presented in Figures 2(b) and 2(c), respectively. The results reveal that in the square I the nanostructure mainly consisted of Zn, Cd, and S and a small amount of Si and O, while in the square II, it is mainly composed of Si and O and tricky amount of S, and there the atomic ratio of Si and O is close to 1 : 2, which is almost consistent with the stoichiometric composition of silicon dioxide. The carbon and copper recorded in the EDS spectra come from the microgrid which was applied to support the samples during TEM characterization. Typical HRTEM image of the 1D nanostructure is shown in Figure 2(d). It is clearly seen that there are pores on the nanostructures, as indicated by Area A circled with dotted line in Figure 2(d). HRTEM image also indicates that there are crystalline (Zn,Cd)S structures (as shown in Area B) and amorphous silica (as shown in Area C) in the nanostructure. In short, the as-prepared porous wire-like structure is a composite material of crystalline ternary (Zn,Cd)S compounds and amorphous silica.

It should be noted that, on checking tens of nanostructures, some of the nanostructures are hollow with thin (Zn,Cd)S/SiO_2 composite films on the inner surface of the shell, indicating they are of tube-like nanostructure, some of the nanostructures have a porous SiO_2 shell with solid (Zn,Cd)S/SiO_2 composite materials in the shell, showing that they are of cable-like nanostructure, and some of the nanostructures have a random mixture of (Zn,Cd)S and SiO_2,
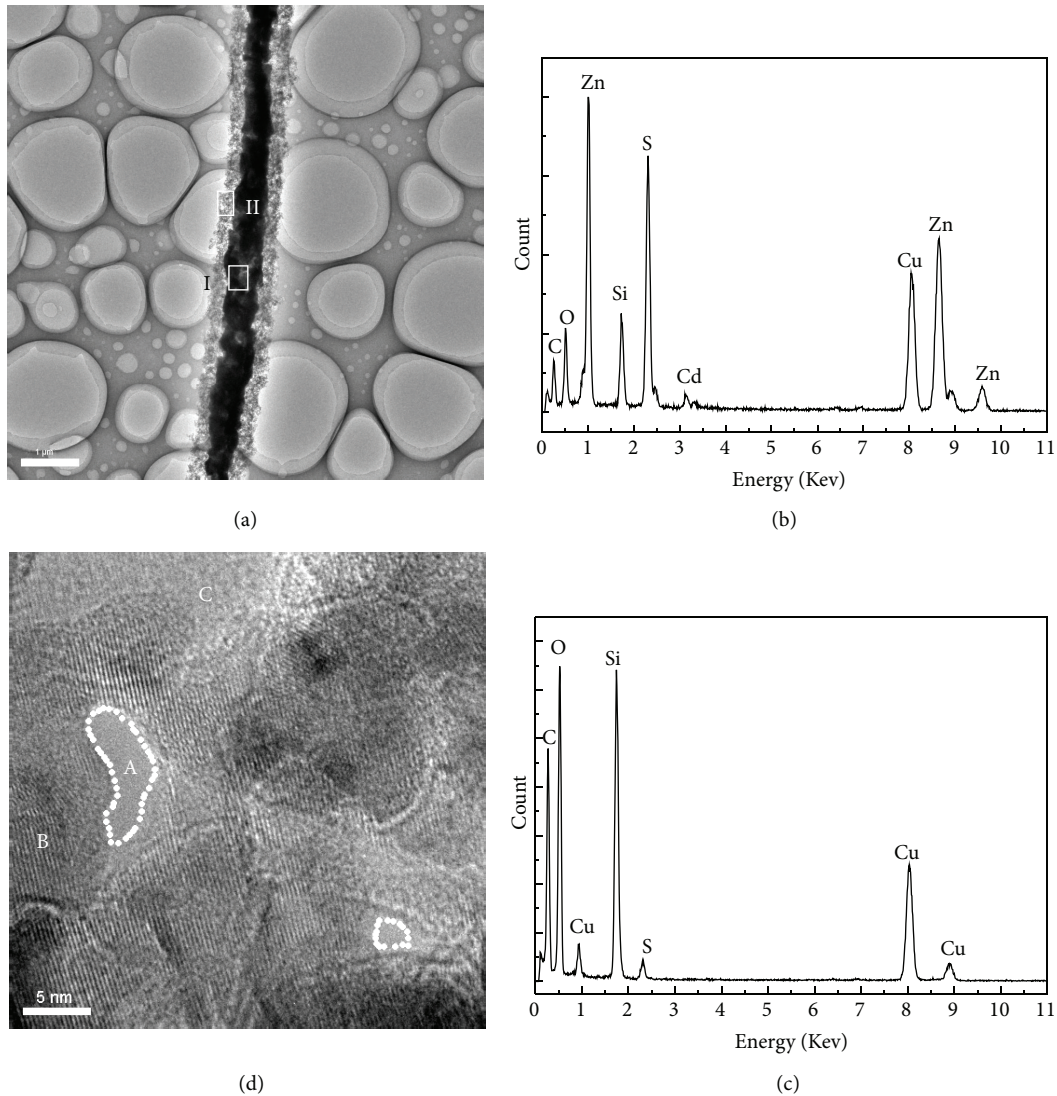
(a)

(b)

(d)

(c)

FIGURE 2: TEM results of the as-synthesized 1D nanostructure: (a) typical TEM image of a single 1D wire-like nanostructure; (b) and (c) EDS spectra taken from the inner as indicated in square I and the outer as indicated in square II of the nanostructure, respectively; and (d) HRTEM image of the nanostructure.

revealing that they are of $(Zn,Cd)S/SiO_2$ nanocomposite wires.

3.2. Growth Mechanism. In the as-prepared 1D nanostructure, amorphous silica was detected. However, during the preparation procedure, no silicon source had been added except the gold coated silicon wafer, so it is sure that the silicon which formed the amorphous silica came from the silicon wafer.

In literature, Elechiguerra et al. [14] had ever reported the preparation of amorphous silica nanowires by using 1:1 Pd/Au coated Si wafer as silicon source and substrate where they collected the products and proposed that the growth of their products is through the classical vapor-liquid-solid (VLS) mechanism on the basis of the observation of eutectic droplets on the tips of their nanowire products. Chen et al. [15] used Ga liquid as catalyst and Si wafer as silicon source,

obtaining amorphous silica nanowires and proposed that the liquid gallium alloy drop only acts as a medium for the formation of silica film, which, as an effective substrate, promotes the oriented growth of silica nanowires by a vapor-solid (VS) growth mechanism. Moreover, Wang et al. [16] had obtained high-porosity ZnO nanowires shelled with Zn_2SiO_4 at the exterior surface by using ZnO as source material and Sn coated Si wafer as substrate and silicon source. In their work, the ZnO nanowires were first formed using a VS process on the Si substrate. Then, SiO vapor sublimated from the Si substrate was deposited on the nanowire surface and diffused into the ZnO lattice, resulting in the formation of Zn_2SiO_4.

In our work, no metal catalytic particles (or contamination) were found on the tips of the 1D $(Zn,Cd)S/SiO_2$ composite nanostructures through the examination of tens of the as-obtained nanostructures by SEM and TEM, implying that the conventional VLS mechanism was not responsible for

the growth of the as-obtained nanostructures. On the other hand, based on our experimental conditions and the observed results shown in Figure 2, we supposed a four-step process, as schematically illustrated in Figure 3, to explain the growth of the as-obtained nanostructures.

In the early stage of the reaction, the temperature was lower than $363°C$ at which gold could form a eutectic alloy with silicon [17], so the Au film broke up and liquid nanodroplets were formed. With the elevation of temperature, these liquid Au droplets might etch the surface of Si substrate to generate some Si vapor surrounding the substrate, after which the Au nanodroplets would absorb Si vapor and oxygen to form $Au-SiO_x$ alloy droplets (the source of oxygen will be discussed later), as shown in Figure 3(b). As the concentration of SiO_x in the alloy droplets becomes oversaturated, solid SiO_x may precipitate out of the alloy droplets and form SiO_2 nanoparticles on the surface of the droplets through homogeneous nucleation in a suitable temperature region. With the proceeding of the reaction, the resultant SiO_2 nanoparticles would lead to the growth of SiO_2 nanowires as reported by Hu et al. [18], which is also schematically illustrated here in Figure 3(c). On the other hand, with the development of SiO_2 nanowires and the increase of system temperature, the source powder mixture of ZnS and CdS would sublimate, and with the carrier gas their vapor flew downstream to the area where SiO_2 nanowires grew. The ZnS and CdS vapor would deposit on the surface of the SiO_2 nanowires due to their high absorptivity, forming ternary (Zn,Cd)S compounds through a VS mechanism. However, (Zn,Cd)S would form textured islands on the surface of SiO_2 nanowires, because they could not form a continuous single-crystalline film due to their large lattice mismatch. Therefore, there are open areas on the SiO_2 surface which are not covered by the (Zn,Cd)S network. In addition, it was reported that the annealing of SiO_2/Si film stacks would lead to the formation of gaseous SiO at temperatures above approximately $800°C$ [19]. Under our experimental temperature, the SiO_2 nanowires which were not covered by the ternary (Zn,Cd)S compounds, might also evaporate out from the surface of the nanowires, leaving pores on the surface of the nanostructures. In fact, we also observed 1D porous SiO_2 nanostructures when silicon wafer was treated under the same experimental conditions only without the evaporation source of ZnS and CdS powder mixture. And some of the newlycome ZnS and CdS vapor might be absorbed into the nanowires through the porous channels, resulting in ternary (Zn,Cd)S compounds inside the nanostructures. And the evaporated SiO vapor from the nanostructures might form new SiO_2 layer on the surface of the nanostructure, resulting in the growth of the nanostructure in radial direction. With the procedure proceeded, porous wire-like $(Zn,Cd)S/SiO_2$ composite nanostructures were finally formed, as shown in Figure 3(d).

The last question is what the source of oxygen was. Considering our experiment conditions, the oxygen that contributed to the formation of SiO_2 nanowires might come from (i) absorbed oxygen in the substrate, (ii) the residual oxygen in the furnace tube due to the low vacuum, (iii) some oxygen contamination in the N_2 gas or (iv) by decomposition
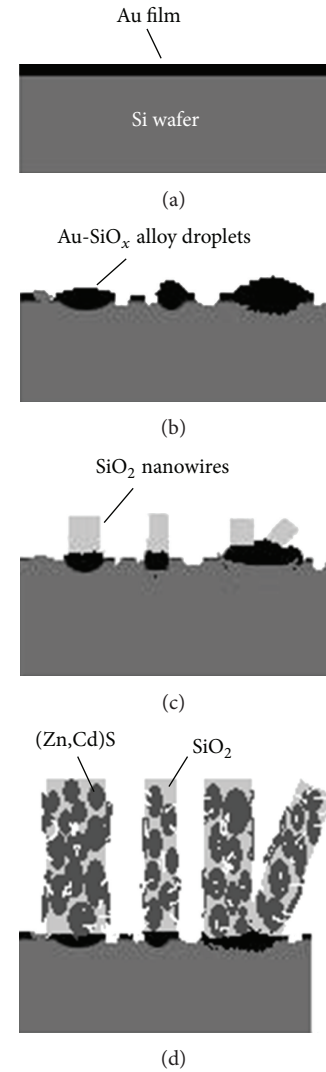

Figure 3: Illustration of the growth mechanism of the as-prepared 1D porous nanostructure: (a) gold film on silicon wafer; (b) $Au-SiO_x$ alloy droplets; (c) formation of SiO_2 nanowires by reaction between silicon and oxygen in the system; and (d) ZnS and CdS vapor deposited on the surface of the SiO_2 nanowires and crystallized to form $(Zn,Cd)S/SiO_2$ composite nanostructure.

of any sort of moisture present in the N_2 gas. Nevertheless, the given temperature in our experiment could only lead to the amorphous silica. In fact, as far as we know, there has been no report so far about the growth of crystalline SiO_2 with or without catalyst at the temperature less than $1300°C$.

3.3. Photoluminescence.

Figure 4(a) shows the PL spectra of the as-prepared $(Zn,Cd)S/SiO_2$ 1D porous nanostructure at 10 K and room temperature using a He-Cd laser with an excitation light of 442 nm. From this figure, one can see that, the PL spectra measured at different temperatures of the prepared nanostructures display a similar broad-band signature, indicating that the photoluminescence of the as-prepared nanostructures is not temperature-dependent. In order to distinguish the attributes of the emission peaks of
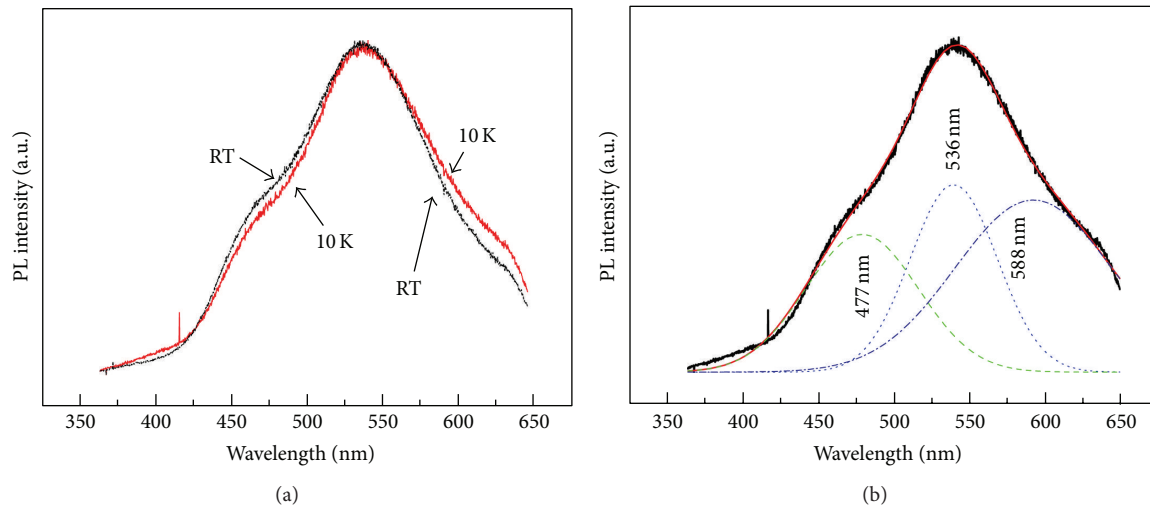
FIGURE 4: The photoluminescence spectra of the as-prepared 1D nanostructures excited with a He-Cd laser (442 nm) at 10 k and room temperature (RT) (a), and the Gaussian fitting of the photoluminescence spectrum obtained at 10 k (b).

the PL spectra, one of the spectra obtained at 10 K was fitted with Gaussian function, and the result was illustrated in Figure 4(b).

In Figure 4(b), the broad emission band at about 536 nm can be excellently fitted into three peaks centered at 477, 536, and 588 nm, respectively. It has been known that ZnS displays a typical emission peak at 366 nm [20] which is attributed to the ultraviolet (UV) excitonic emission, and CdS displays a typical emission peak at 525 nm [21] which was designated to the near band edge emission. As a result of fine tuning of electronic properties, the emission of the as-synthesized ternary (Zn,Cd)S nanomaterials is just between both of them, so we suppose that the stable emission peak centered at 477 nm is attributed to the band edge emission of the ternary (Zn,Cd)S compounds [9]. From literature, we also suggest that the emission peak centered at 536 nm is correspondent to the neutral oxygen vacancies of the amorphous silica [18, 22], and the emission peak centered at 588 nm is assigned to antisymmetric stretching of Si–O–Si and non-stoichiometric SiO_x $(1 < x < 2)$ [23].

4. Conclusions

Wire-like $(Zn,Cd)S/SiO_2$ composite nanostructural materials were successfully synthesized with a one-step evaporation of mixed ZnS and CdS powders onto a silicon wafer coated with gold film. The microstructure characterizations show that the 1D $(Zn,Cd)S/SiO_2$ composite materials are of porous structure. The photoluminescence spectra of the 1D composite nanostructures recorded at different temperatures present the similar broad emission band around 536 nm, which can be fitted by Gaussian function into three emission peaks centered at 477, 536, and 588 nm, and attributed to band edge emission of the ternary (Zn,Cd)S compounds, neutral oxygen vacancies of the amorphous silica, and antisymmetric stretching of Si–O–Si and nonstoichiometric SiO_x $(1 < x < 2)$, respectively.

Conflict of Interests

The authors declare that there is no conflict of interests regarding the publication of this paper.
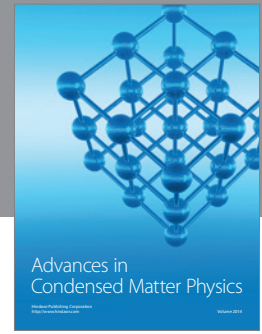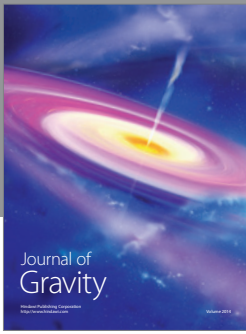
Acknowledgments

References

[1] X.-P. Shen, A.-H. Yuan, F. Wang, J.-M. Hong, and Z. Xu, "Fabrication of well-aligned CdS nanotubes by CVD-template method," *Solid State Communications*, vol. 133, no. 1, pp. 19–22, 2005.

[2] J. Zhang, F.-H. Jiang, and L.-D. Zhang, "Fabrication of single-crystalline semiconductor CdS nanobelts by vapor transport," *Journal of Physical Chemistry B*, vol. 108, no. 22, pp. 7002–7005, 2004.

[3] D.-S. Kim, Y.-J. Cho, J.-H. Park, J. Yoon, Y. Jo, and M.-H. Jung, "(Mn, Zn)Co-doped CdS nanowires," *Journal of Physical Chemistry C*, vol. 111, no. 29, pp. 10861–10868, 2007.

[4] C.-H. Ye, G.-W. Meng, Y.-H. Wang, Z. Jiang, and L. Zhang, "On the growth of CdS nanowires by the evaporation of CdS nanopowders," *Journal of Physical Chemistry B*, vol. 106, no. 40, pp. 10338–10341, 2002.

[5] Y.-T. Chen, J.-B. Ding, Y. Guo, L.-B. Kong, and H.-L. Li, "A facile route to preparation of CdS nanorods," *Materials Chemistry and Physics*, vol. 77, no. 3, pp. 734–737, 2003.

[6] Q. Q. Wang, G. L. Zhao, and G. R. Han, "Synthesis of single crystalline CdS nanorods by a PVP-assisted solvothermal method," *Materials Letters*, vol. 59, no. 21, pp. 2625–2629, 2005.

[7] Y. Li, J.-H. Wan, and Z.-N. Gu, "The formation of cadmium sulfide nanowires in different liquid crystal systems," *Materials Science and Engineering A*, vol. 286, no. 1, pp. 106–109, 2000.

[8] D. Routkevitch, T. Bigioni, M. Moskovits, and J. M. Xu, "Electrochemical fabrication of CdS nanowire arrays in porous anodic aluminum oxide templates," *Journal of Physical Chemistry*, vol. 100, no. 33, pp. 14037–14047, 1996.

[9] H.-J. Liu and Y.-C. Zhu, "Synthesis and characterization of ternary chalcogenide ZnCdS 1D nanostructures," *Materials Letters*, vol. 62, no. 2, pp. 255–257, 2008.

[10] R. Venugopal, P. Lin, and Y. Chen, "Photoluminescence and Raman scattering from catalytically grown $Zn_xCd_{1-x}Se$ alloy nanowires," *Journal of Physical Chemistry B*, vol. 110, no. 24, pp. 11691–11696, 2006.

[11] T.-Y. Lui, J.-A. Zapien, H. Tang et al., "Photoluminescence and photoconductivity properties of copper-doped $Cd_{1-x}Zn_xS$ nanoribbons," *Nanotechnology*, vol. 17, no. 24, pp. 5935–5940, 2006.

[12] V. I. Kozlovskii, D. A. Sannikov, and D. E. Sviridov, "Nanoscale ZnCdS/ZnSSe heterostructures for semiconductor lasers," *Bulletin of the Lebedev Physics Institute*, vol. 35, no. 2, pp. 35–39, 2008.

[13] M. Kobayashi, J. Ueno, M. Enami et al., "Growth and UV-A sensor applications of MgCdS/ZnCdS superlattices," *Journal of Crystal Growth*, vol. 278, no. 1–4, pp. 273–277, 2005.

[14] J. L. Elechiguerra, J.-A. Manriquez, and M. J. Yacaman, "Growth of amorphous SiO_2 nanowires on Si using a Pd/Au thin film as a catalyst," *Applied Physics A*, vol. 79, no. 3, pp. 461–467, 2004.

[15] Y.-Q. Chen, Q.-T. Zhou, H.-F. Jiang et al., "Aligned silica nanowires on the inner wall of bubble-like silica film: the growth mechanism and photoluminescence," *Nanotechnology*, vol. 17, no. 4, pp. 1022–1025, 2006.

[16] X.-D. Wang, C.-J. Summers, and Z.-L. Wang, "Mesoporous single-crystal ZnO nanowires epitaxially sheathed with Zn_2SiO_4," *Advanced Materials*, vol. 16, no. 14, pp. 1215–1218, 2004.

[17] P. K. Sekhar, N. S. Ramgir, R. K. Joshi, and S. Bhansali, "Selective growth of silica nanowires using an Au catalyst for optical recognition of interleukin-10," *Nanotechnology*, vol. 19, no. 24, Article ID 245502, 18 pages, 2008.

[18] J. Q. Hu, Y. Jiang, X.-M. Meng, C.-S. Lee, and S.-T. Lee, "A simple large-scale synthesis of very long aligned silica nanowires," *Chemical Physics Letters*, vol. 367, no. 3-4, pp. 339–343, 2003.

[19] F. M. Kolb, A. Berger, H. Hofmeister, E. Pippel, U. Gösele, and M. Zacharias, "Periodic chains of gold nanoparticles and the role of oxygen during the growth of silicon nanowires," *Applied Physics Letters*, vol. 89, no. 17, Article ID 173111, 2006.

[20] Y.-Q. Chang, M.-W. Wang, X.-H. Chen, S. Ni, and W. Qiang, "Field emission and photoluminescence characteristics of ZnS nanowires via vapor phase growth," *Solid State Communications*, vol. 142, no. 5, pp. 295–298, 2007.

[21] S. Kar, B. Satpati, P. V. Satyam, and S. Chaudhuri, "Synthesis and optical properties of CdS nanoribbons," *Journal of Physical Chemistry B*, vol. 109, no. 41, pp. 19134–19138, 2005.

[22] H. Nishikawa, T. Shiroyama, R. Nakamura, Y. Ohki, K. Nagasawa, and Y. Hama, "Photoluminescence from defect centers in high-purity silica glasses observed under 7.9-eV excitation," *Physical Review B*, vol. 45, no. 2, pp. 586–591, 1992.

[23] I. K. Battisha, H. H. Afify, and Y. Badr, "Structural and photoluminescence behaviors of nano-structure thin film and bulk silica gel derived glasses," *Journal of Sol-Gel Science and Technology*, vol. 25, no. 1, pp. 5–15, 2002.